

SPECIFICATION OF 500-MB. PARAMETERS BY DOWNWARD EXTRAPOLATION¹

MAURICE E. GRAVES

Department of Aerospace Engineering, The University of Michigan, Ann Arbor, Mich.

and

EDWARD S. EPSTEIN

Department of Meteorology and Oceanography, The University of Michigan, Ann Arbor, Mich.

ABSTRACT

With the future utilization of new-type upper tropospheric observations in mind, the estimation of 500-mb. geopotential height from 300-mb. data is accomplished by least squares regression. The regression coefficients form latitudinal patterns which can be expressed by linear relationships in low latitudes and parabolic relationships elsewhere. From three year's mid-seasonal-month grid data, measures of extrapolation error are obtained over half of the Northern Hemisphere. Verifying tests with radiosonde station data indicate that the error in low latitudes is substantially due to analysis noise in the 500-mb. grid data.

When the same techniques are applied to 200-mb. information, further error studies show considerably less feasibility of extrapolation from that level to 500 mb. However, the temperature at 200 mb. is found to be valuable in predicting the simultaneous temperature at 500 mb.

1. INTRODUCTION

Throughout the history of the radiosonde, there have been attempts to extrapolate data upward to permit the analysis of higher levels. Some of these recent efforts extend into the lower stratosphere, and are described by Teweles and Snidero [12], Finger, Woolf, and Anderson [3], and Spiegler, Veigas, and Rahn [11]. Concurrently, objective analysis schemes have been proposed stressing optimum interpolation, as by Gandin [5]; generation of polynomial surfaces, as by Gilchrist and Cressman [6], Johnson [7], Koss [8], and Panofsky [10]; and the use of preliminary field estimates, as by Bergthorsson and Döös [1] and Cressman [2]. Although these various methods are designed to utilize radiosonde data above and well away from the balloon's path, vast data voids still remain, unrepresented by dependable observational information on the atmospheric structure parameters.

To fill these voids, new techniques of measurement are being developed. One such technique [9] is based upon the monitoring of signals from instrumented constant-density balloons. Another, detailed by Fischbach [4], involves the satellite-tracking of star images as they are refracted by the atmosphere during occultation. However, in their present states of development, both of these schemes have serious problems in procuring data at the 500-mb. level which is so crucial to weather forecasting. In the case of the constant-density balloons, icing loads

may force the probes down, while refraction scans have to contend with cloud obstruction. On the other hand, both techniques would provide abundant data at 200 mb. and somewhat smaller quantities at 300 mb.

In view of the profitable operational use of extrapolation methods from 500 mb. upward in the past, vertical extrapolation in the opposite sense should be feasible. The feasibility is studied here by evaluation of the errors in 500-mb. geopotential height and temperature when linear regression equations are formed for the 300-500-mb. and 200-500-mb. layers, and some convenient and effective relationships between latitude and the various regression coefficients are obtained.

2. ESTIMATION OF THE 500-MB. HEIGHT

The hypsometric formula suggests that knowledge of the mean temperature within a layer and the height of the upper boundary is sufficient to determine the height of the lower boundary. If the mean layer temperature is unknown, the temperature at the top is an indicator of the thermal conditions within the layer, and it is reasonable to estimate the height of the lower boundary by a linear regression equation, i.e.,

$$h_{500} = b_1 + b_2 h_{300} + b_3 T_{300} \quad (1)$$

where h_{500} = geopotential height at 500 mb. (ft.); h_{300} = geopotential height at 300 mb. (ft.); T_{300} = temperature at 300 mb. (°C.); and b_1, b_2, b_3 = least squares regression coefficients.

¹ Publication No. 120, Department of Meteorology and Oceanography, The University of Michigan.

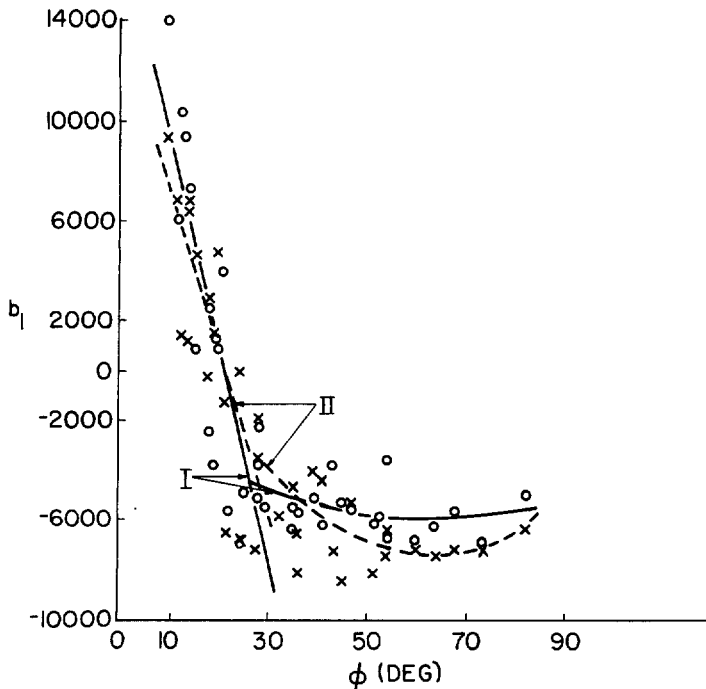


FIGURE 1.—Computed least squares regression coefficients, b_1 , at each grid point in Quadrant I (circles) and in Quadrant II (crosses). The curves marked I (II) are least squares fits for Quadrant I (II) by equation (4). Data used are for January (1956, 1957, 1958).

We have computed such coefficients for a sizable sample of data. The data used are Project 433L grid data for January, April, and July (1956, 1957, 1958) and October (1955, 1956, 1957). This information is available at the National Weather Records Center on punched cards, having been taken from NAWAC hemispheric charts. Two quadrants encompassing the eastern Pacific Ocean and North America (Quadrant I), and the Atlantic Ocean and western Europe (Quadrant II) were selected for evaluation, and a 36-point grid (fig. 4) was set up in each quadrant for the purposes of the investigation. With two analyses per day, each 30-day month is thus represented by 180 interpolated grid values per point.

Regression coefficients for January, for each of the quadrants, are plotted against latitude, ϕ , in figures 1-3. It may be seen that b_2 increases from 0° to 30° N., whereas b_1 and b_3 decrease in this latitudinal zone; at higher latitudes these variations are less pronounced and they may show reversals. These are typical variations of the coefficients in all seasons. Differences between the two quadrants are more pronounced in other seasons.

The regularity of the variation with latitude of the regression coefficients suggests they may be represented by simple functions of latitude, ϕ . Three types of functional relationships were tried in fitting the points in figures 1-3:

$$b_j = a_{1j} + a_{2j} \sin \phi + a_{3j} \cos \phi \quad (0^\circ \leq \phi \leq 90^\circ, j=1, 2, 3) \quad (2)$$

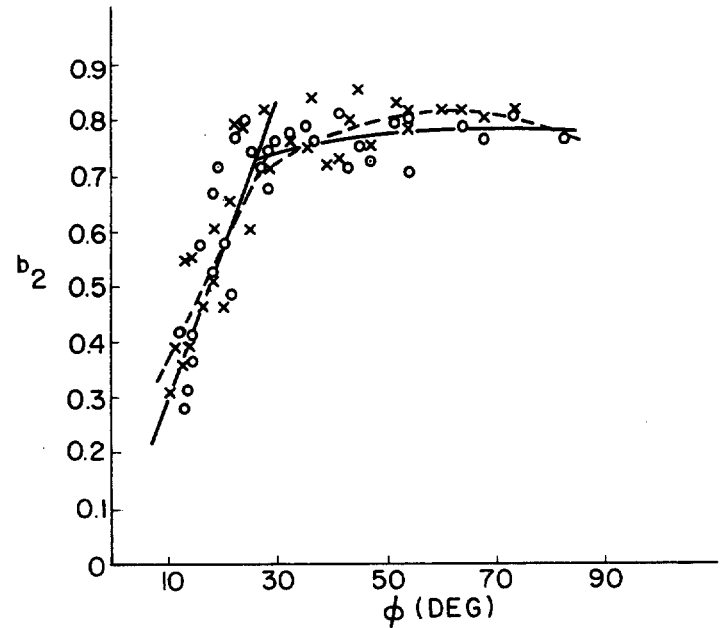


FIGURE 2.—Computed least squares regression coefficients, b_2 . See legend for figure 1.

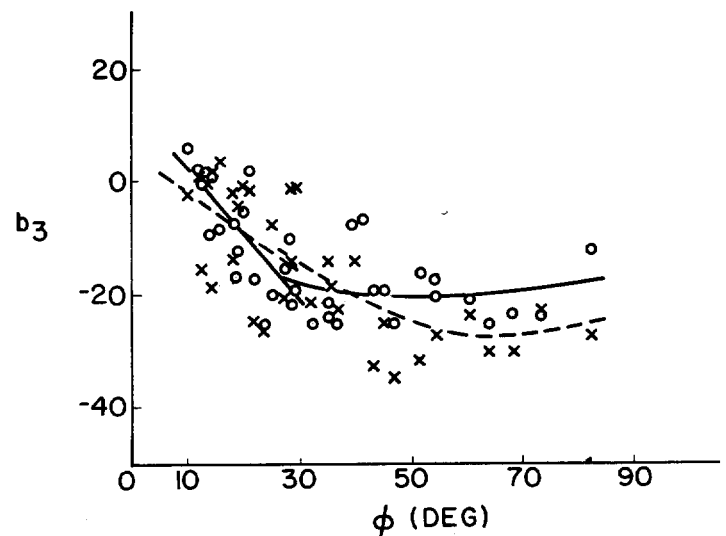


FIGURE 3.—Computed least squares regression coefficients, b_3 . See legend for figure 1.

$$b_j = a'_{1j} + a'_{2j} \phi + a'_{3j} \phi^2 \quad (0^\circ \leq \phi \leq 90^\circ, j=1, 2, 3) \quad (3)$$

$$b_j = \begin{cases} c_{1j} + c_{2j} \phi & (0^\circ \leq \phi < 28^\circ, j=1, 2, 3) \\ d_{1j} + d_{2j} \phi + d_{3j} \phi^2 & (28^\circ \leq \phi \leq 90^\circ, j=1, 2, 3) \end{cases} \quad (4)$$

Equation (4) was found to be superior to equations (2) and (3) in all seasons. In evaluating the c_j and d_j , an overlap between 28° N. and 30° N. was introduced to reduce

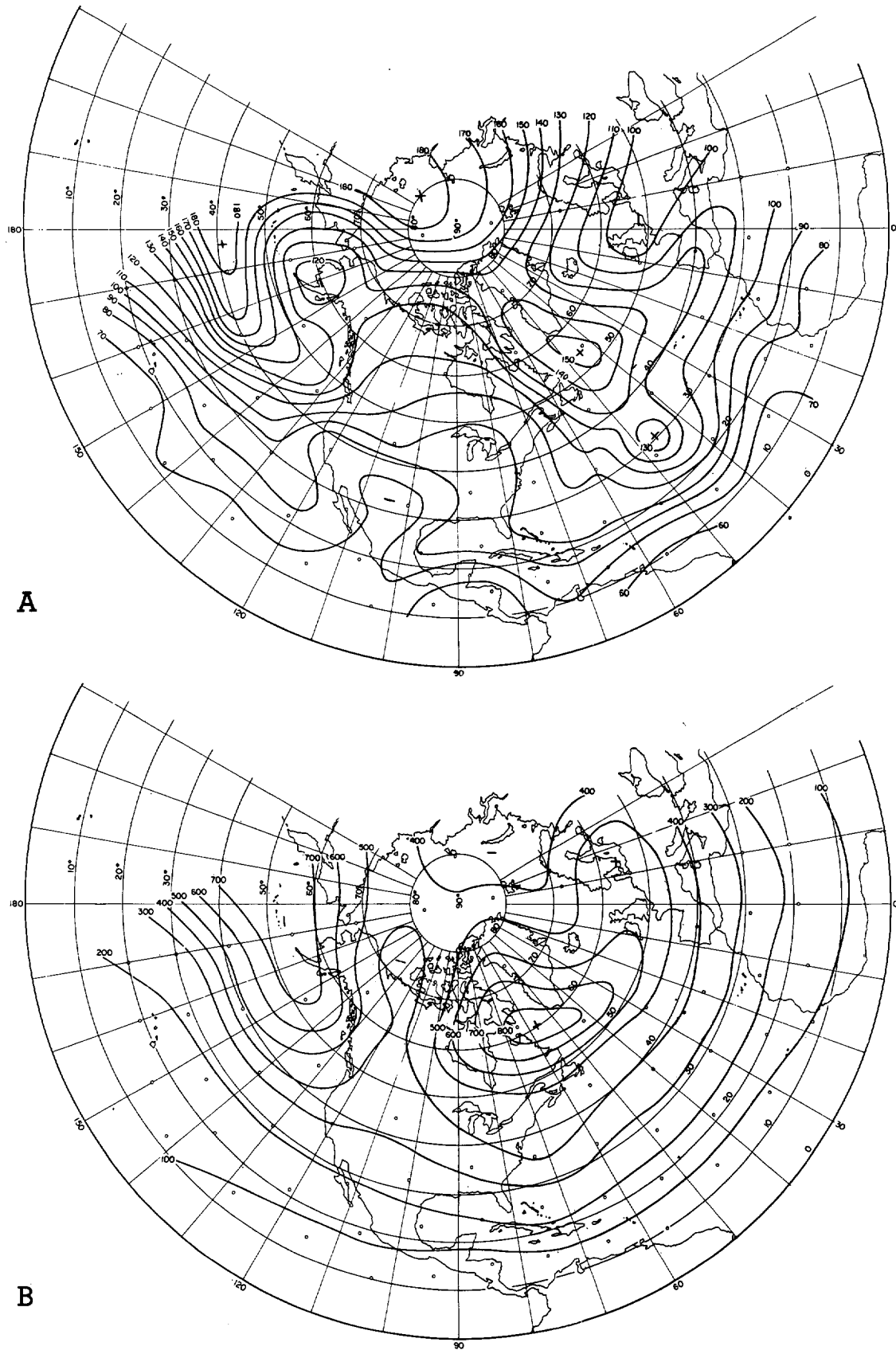


FIGURE 4.—(A) Standard error of estimate in feet for the regression from 300 mb. to 500 mb. to obtain geopotential height, e.g., h_{300} , T_{300} to h_{500} . Computations are made at grid points (circles). Quadrants join at 80° W. Data are for January (1956, 1957, 1958). Plus and minus symbols denote relative maxima and minima. (B) Standard deviation of 500-mb. geopotential height in feet for grid points in figure 4a.

TABLE 1.—Least squares regression coefficients for linear curve-fitting (c_1) and parabolic curve-fitting (d_1) for mid-seasonal months. Regression is from 300 mb. to 500 mb. to obtain geopotential height, e.g., $h_{300}, T_{300} \rightarrow h_{500}$. Two degrees of overlap (28° N. to 30° N.) are used in computing coefficients. Data used are for October 1955 to July 1958

Coefficient	Month	c_1	c_2	d_1	d_2	d_3
Quadrant I						
b_1	Jan.	18834	-879.6	-1513	-142.5	1.124
b_1	Apr.	16509	-689.6	-6240	73.7	-0.798
b_1	July	20415	-598.9	28106	-1064.9	8.307
b_1	Oct.	22308	-861.9	8570	-535.4	4.969
b_2	Jan.	0.0243	0.0267	0.6522	0.00383	-0.000024
b_2	Apr.	.0925	.0212	.8128	-.00324	.000034
b_2	July	-.0392	.0188	-.2114	.03053	-.000236
b_2	Oct.	-.0760	.0260	.3637	.01524	-.000144
b_3	Jan.	13.76	-1.16	-8.52	-0.428	0.00379
b_3	Apr.	8.51	-0.71	-8.21	-0.263	0.00215
b_3	July	1.19	-0.28	52.88	-2.512	.02137
b_3	Oct.	22.10	-1.29	21.02	-1.533	.01344
Quadrant II						
b_1	Jan.	14294	-660.6	4810	-390.0	3.100
b_1	Apr.	18517	-660.6	12545	-692.2	6.369
b_1	July	20717	-570.4	23569	-970.6	8.129
b_1	Oct.	19684	-707.7	9707	-562.0	5.052
b_2	Jan.	0.1594	0.0205	0.4786	0.01079	-0.000087
b_2	Apr.	.0416	.0198	-.2342	.02029	-.000188
b_2	July	-.0507	.0181	-.0860	.02829	-.000237
b_2	Oct.	-.0107	.0220	.3233	.01627	-.000148
b_3	Jan.	5.56	-0.72	17.25	-1.369	0.01037
b_3	Apr.	16.65	-0.94	19.95	-1.530	.01380
b_3	July	-5.40	0.02	31.60	-1.693	.01438
b_3	Oct.	3.14	-0.37	18.60	-1.405	.01206

TABLE 2.—Standard error of estimate for each January for Quadrant II, using b_1 (ϕ) relationship. Upper grouping is for linear fit ($\phi < 28^\circ$ N.), lower grouping is for parabolic fit ($\phi \geq 28^\circ$ N.). Regression and data are same as in table 1

Lat.	Long.	1956	1957	1958	Mean
10.4° N.	57.2° W.	50 ft.	54 ft.	73 ft.	59 ft.
12.5	18.6	87	60	84	77
13.2	65.9	62	77	71	70
13.9	45.0	72	77	74	74
14.7	75.2	85	82	59	75
14.7	31.6	70	59	75	68
16.3	10.0	91	61	80	77
18.8	53.5	85	112	77	91
18.8	0.3	103	74	105	94
19.6	10.0° E.	109	74	96	93
20.5	23.7° W.	83	71	72	75
21.5	38.9	84	106	120	103
22.4	63.3	96	123	64	94
24.4	74.3	91	110	77	93
25.5	14.0	103	84	99	95
27.7	48.0	127	138	118	128
28.8	30.6	104	86	121	104
28.8	2.5	114	105	95	105
30.0	10.0° E.	112	104	97	105
32.6	59.5° W.	97	99	106	101
35.7	72.9	93	91	95	93
35.7	19.7	108	98	140	115
36.8	40.0	99	101	147	116
39.9	6.0	134	146	80	120
41.7	10.0° E.	91	115	93	100
43.5	53.5° W.	118	129	149	132
45.4	28.7	116	153	119	129
47.4	70.5	97	106	88	97
51.9	11.8	90	113	99	101
54.5	43.1	165	151	139	152
54.5	10.0° E.	87	97	101	95
60.4	66.0° W.	123	101	116	113
64.0	23.7	146	129	133	136
68.2	10.0° E.	138	98	142	126
73.7	53.5° W.	144	125	158	142
82.7	10.0° E.	185	159	142	162

the discontinuity between the linear and parabolic segments. These coefficients are listed for the mid-seasonal months in table 1. The root mean square errors, ϵ , of the estimates of h_{500} , using in equation (1) coefficients evaluated with equation (4), were computed. The January results for Quadrant II are given in table 2 and those for both quadrants are plotted in figure 4a. The patterns show that the effectiveness of h_{300} and T_{300} in predicting h_{500} is greatest in moderately high latitudes, decreasing somewhat in polar regions and falling off seriously near the Equator. Values of ϵ range up to 200 ft. However, over much of the area within the two quadrants, the mean ϵ for January (fig. 4a) is under 150 ft. Indeed, these errors of estimate are quite small compared to s , the standard deviation of h_{500} (fig. 4b), everywhere but in low latitudes. This is also true in the other mid-seasonal months, even though s decreases to a summer minimum.

ϵ is compared with the rms error for the 12-hr., 24-hr., and 36-hr. persistence estimates in figure 5a (for January) and 5b (for July). One standard deviation, s , of h_{500} is also shown in these figures. In January, the values of h_{500} obtained by regression from 300-mb. data are found to be more accurate than 24-hr. persistence estimates at all latitudes investigated, and above 25° N. they are more accurate than 12-hr. persistence. In July, the extrapolated values have a 10 to 20 percent decrease in their standard error of estimate, but the various persistence estimate errors and the standard deviation of h_{500} are considerably smaller. This reduces the advantage of regression estimates over persistence in summer.

The increase in error imposed by the use of equation (4) instead of the directly computed regression coefficients is illustrated in figure 6. The ratio, R^2 , of the explained variance to the total variance of h_{500} is plotted against latitude. R is the multiple correlation coefficient for the estimates of h_{500} . The solid curve is based on coefficients computed directly from equation (1), and the dashed curve is based on computations using (4). The two curves are sufficiently close together to justify the use of the linear and parabolic approximations to the regression coefficients at grid points (figs. 1-3). Operationally, it may be feasible to combine quadrants if the resulting increase in ϵ is acceptable or if the differences between the relevant coefficients do not prove to be statistically significant. The discontinuities at the intersections of the linear and parabolic segments (figs. 1-3) are found to be less troublesome than the discontinuities commonly encountered in assigning particular regression coefficients to latitudinal bands several degrees in width.

The accuracy of such a procedure is bound to deteriorate as one goes to thicker layers. The computations were repeated, using as independent variables the height and temperature at 200 mb. These regression coefficients are listed in table 3 and the resulting errors ϵ for January, Quadrant II, are given in table 4. A few of the errors listed in the latter table exceed 200 ft., but at most mid- and high-latitude grid points 100 ft. $< \epsilon < 200$ ft. A graph of R^2 (fig. 7) shows a general decrease over figure 6 at all latitudes. With the possible exception of the polar region, the proximity of the two curves in figure 7 in-

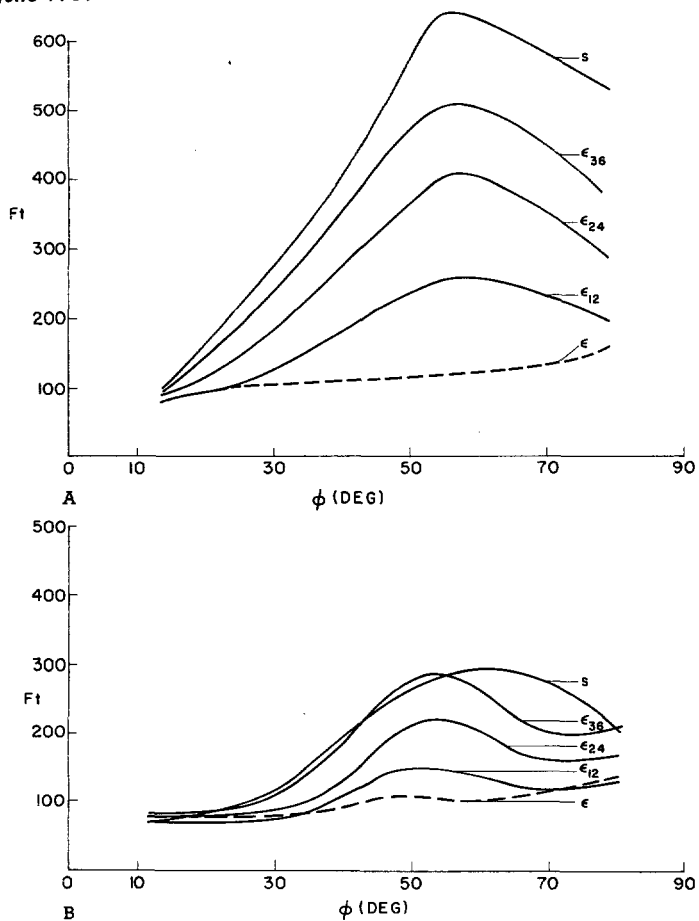


FIGURE 5.—Standard error of estimate, ϵ , for the regression from 300 mb. to 500 mb., e.g., h_{300} , T_{300} to h_{500} , using the relationship between b_j and ϕ ; rms error for 12-hr. persistence (ϵ_{12}), 24-hr. persistence (ϵ_{24}), and 36-hr. persistence (ϵ_{36}) in estimating h_{300} ; and standard deviation, s , of h_{500} . (A) Data for January (1956, 1957, 1958), Quadrant II. (B) Data for July (1956, 1957, 1958), Quadrant II.

indicates that the use of latitude as a single independent variable in computing the b_j and h_{500} is a satisfactory method in this case, also.

The distribution of errors at a number of grid points was studied by the use of histograms (not shown). January data yield Gaussian features at all latitudes when the layer from 300 mb. to 500 mb. is extrapolated with grid point coefficients. The $b_j(\phi)$ relationship, equation (4), often introduces some skewness, although ϵ is not increased markedly (table 2). The regression from 200 mb. to 500 mb. gives rather flat error histograms at all latitudes. Extreme errors in estimating h_{500} , e.g., those apparently related to the occurrence of the tropopause within the layer, rarely exceed 300 ft. in the shallower layer. However, in the thicker layer very large extrapolation errors are occasionally encountered.

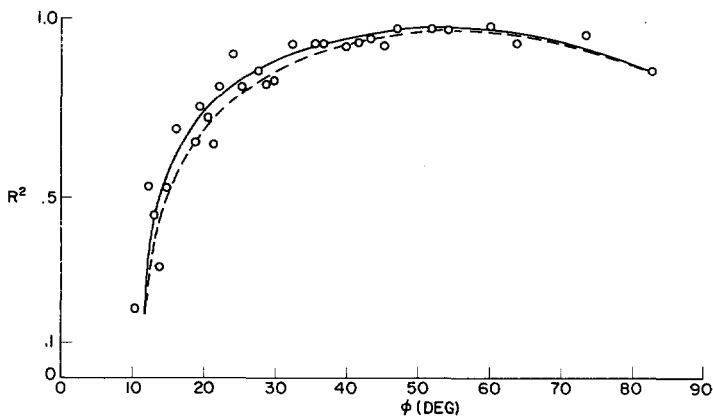


FIGURE 6.—Ratio, R^2 , of explained variance to total variance of 500-mb. geopotential height. Circles are average values of R^2 for all grid points at the latitude indicated. Solid line is a visual fit of the circles. Broken line is a visual fit of R^2 resulting from use of the relationship between the b_j and ϕ . The regression is from 300 mb. to 500 mb. Data are for January (1956, 1957, 1958), both quadrants.

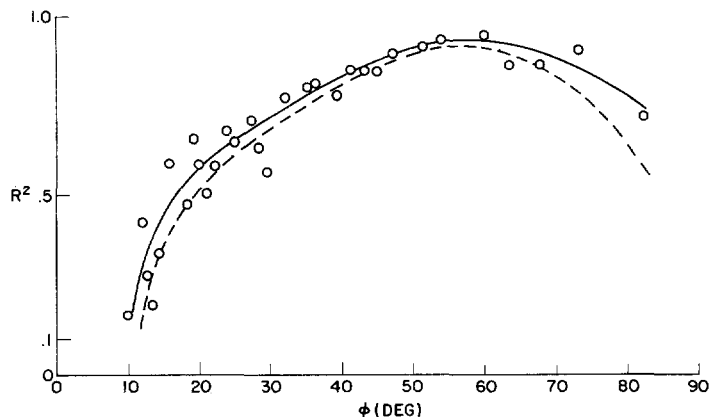


FIGURE 7.—See legend for figure 5. The regression is from 200 mb. to 500 mb.

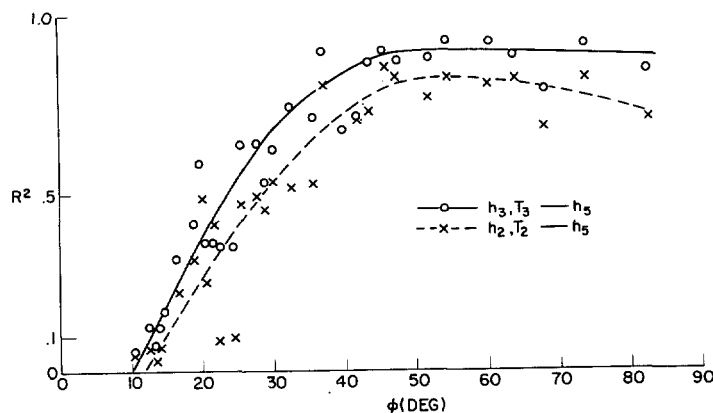


FIGURE 8.—Ratio, R^2 , of explained variance to total variance of 500-mb. geopotential height. Circles are for regression from 300 mb. to 500 mb., crosses for regression from 200 mb. to 500 mb. Values of R^2 are averaged over all grid points at the latitude indicated. Data are for July (1956, 1957, 1958), Quadrant I.

TABLE 3.—Same as table 1, except regression is from 200 mb. to 500 mb. Five degrees of overlap (25° N. to 30° N.) are used in computing coefficients

Coefficient	Month	c ₁	c ₂	d ₁	d ₂	d ₃
Quadrant I	b ₁ Jan.	19857	-777.4	26498	-1219.9	9.914
	b ₁ Apr.	22703	-827.1	4382	-213.2	0.042
	b ₁ July	24893	-662.1	8146	-48.2	-2.256
	b ₁ Oct.	21239	-897.1	17874	-801.5	6.884
	b ₂ Jan.	-0.0078	0.0184	-0.1976	0.03051	-0.000250
	b ₂ Apr.	-0.0689	.0193	.3489	.00545	-0.00005
	b ₂ July	-1.338	.0159	.3042	-.00038	.000067
	b ₂ Oct.	-0.0383	.0165	.0857	-.01686	-.000146
	b ₃ Jan.	7.00	-0.84	7.03	-0.654	0.00341
	b ₃ Apr.	14.48	-0.92	-19.83	0.483	-.00894
	b ₃ July	6.29	-0.41	9.82	-0.596	.00220
	b ₃ Oct.	11.21	-0.80	39.17	-2.265	-.01859
Quadrant II	b ₁ Jan.	21269	-915.3	8543	-554.8	4.385
	b ₁ Apr.	17251	-461.0	23554	-911.3	5.999
	b ₁ July	17183	-479.2	16222	-533.5	3.602
	b ₁ Oct.	22628	-702.3	21864	-858.9	6.275
	b ₂ Jan.	-0.0343	0.0216	0.2711	0.01301	-0.000105
	b ₂ Apr.	.0628	.0104	-.0986	.02134	-.000137
	b ₂ July	.0263	.0123	.0747	.01306	-.000083
	b ₂ Oct.	-.0855	.0172	-.0078	.01828	-.000130
	b ₃ Jan.	14.88	-0.95	12.26	-0.935	0.00619
	b ₃ Apr.	8.91	-0.69	9.69	-0.941	.00840
	b ₃ July	-18.30	0.21	-11.52	-0.031	.00063
	b ₃ Oct.	-1.76	-0.11	43.18	-2.210	.01836

TABLE 4.—Same as table 2, except regression is from 200 mb. to 500 mb

Lat.	Long.	1956	1957	1958	Mean
10.4° N.	57.2° W.	58 ft.	55 ft.	63 ft.	60 ft.
12.5	18.6	84	67	89	80
13.2	65.9	81	62	61	68
13.9	45.0	78	72	66	72
14.7	75.2	115	69	46	77
14.7	31.6	77	60	65	67
16.3	10.0	123	73	89	95
18.8	53.5	126	82	80	96
18.8	0.3	150	94	115	120
19.6	10.0° E.	152	114	124	130
20.5	23.7° W.	102	84	95	94
21.5	38.9	127	90	121	113
22.4	63.3	161	101	114	125
24.4	74.3	205	93	190	163
25.5	14.0	136	115	153	135
27.7	48.0	163	124	149	145
28.8	30.6	145	152	133	143
28.8	2.5	137	134	117	129
30.0	10.0° E.	138	140	135	138
32.6	59.5° W.	142	156	198	165
35.7	72.9	169	152	232	184
35.7	19.7	164	150	162	159
36.8	40.0	133	160	191	162
39.9	6.0	184	170	166	173
41.7	10.0° E.	160	174	138	157
43.5	53.5° W.	182	225	210	206
45.4	28.7	206	207	181	198
47.4	70.5	157	149	149	152
51.9	11.8	160	202	202	188
54.5	43.1	202	218	196	205
54.5	10.0° E.	162	189	198	183
60.4	66.0° W.	246	159	161	189
64.0	23.7	231	176	219	209
68.2	10.0° E.	229	193	231	218
73.7	53.5° W.	225	134	218	192
82.7	10.0° E.	261	221	177	220

The standard deviation of h_{500} and the standard error of estimate by regression both have their maxima in winter and minima in summer. Values of R^2 for July, Quadrant I, are plotted in figure 8. Some loss of accuracy in summer is noted, especially south of 45° latitude.

TABLE 5.—Standard error of estimate, ϵ , and ratio R^2 of explained variance to total variance of 500-mb. geopotential height for selected radiosonde stations. Columns headed ϵ_1 and R_1^2 are based on the use of station regression coefficients, those headed ϵ_2 and R_2^2 are based on the relationship between b_1 and latitude. Regression layers are as indicated. N = number of observations. Data are for January (1956, 1957, 1958)

Station	Lat. (°N.)	N	$h_{300}, T_{300} \rightarrow h_{500}$				$h_{200}, T_{200} \rightarrow h_{500}$			
			ϵ_1	R_1^2	ϵ_2	R_2^2	ϵ_1	R_1^2	ϵ_2	R_2^2
Mazatlan	23.2	41	29 ft.	0.964	44 ft.	0.923	51 ft.	0.890	80 ft.	0.747
Miami	25.9	176	54	.952	65	.928	129	.716	151	.614
San Diego	32.7	169	51	.958	52	.953	108	.813	115	.768
Greensboro	36.1	185	66	.975	67	.969	133	.890	174	.793
Buffalo	43.0	296	75	.967	78	.955	130	.875	151	.830
Boise	43.6	174	75	.960	98	.942	118	.902	124	.892
Moosonee	51.2	144	86	.979	88	.975	149	.932	156	.921
Edmonton	53.6	181	81	.950	90	.946	123	.920	126	.895
McGrath	63.0	156	92	.978	94	.977	143	.945	168	.934
Frobisher	63.7	133	96	.986	100	.985	158	.961	179	.953
Coppermine	67.8	135	90	.946	96	.940	160	.820	185	.777

TABLE 6.—Standard deviation of temperature at 500 mb., $s(T_{500})$, and error data for selected radiosonde stations. ϵ_1 (ϵ_2) is the standard error of estimate for the regression $h_{300}, T_{300} \rightarrow T_{500}$ ($h_{200}, T_{200} \rightarrow T_{500}$). R_1^2 is the ratio of explained variance to total variance of T_{500} for the 4-dimensional regression

Station	$s(T_{500})$	ϵ_1	ϵ_2	R_1^2
Balboa	1.7° C.	1.6° C.	1.1° C.	0.582
Mazatlan	2.3	1.7	1.1	.771
Miami	2.4	2.4	1.4	.660
San Diego	3.2	2.8	1.7	.718
Greensboro	4.3	3.8	2.0	.784
Buffalo	5.1	5.0	2.2	.814
Boise	5.2	4.8	2.1	.837
Moosonee	7.0	5.6	2.3	.892
Edmonton	6.9	6.0	4.0	.664
McGrath	5.5	5.2	2.5	.793
Frobisher	8.1	7.1	3.0	.863
Coppermine	5.9	4.8	2.7	.791

TABLE 7.—Standard error of estimate, ϵ , and ratio, R^2 , of explained variance to total variance for various regressions including surface pressure as a predictor. The subscripts on ϵ and R^2 indicate the regression in accordance with the following key: 1= $h_{200}, T_{200}, p_0 \rightarrow T_{500}$, 2= $h_{300}, T_{300}, p_0 \rightarrow h_{500}$, 3= $h_{200}, T_{200}, p_0 \rightarrow h_{500}$. N = number of observations. Data are for January (1956, 1957, 1958)

Station	N	ϵ_1	R_1^2	ϵ_2	R_2^2	ϵ_3	R_3^2
Greensboro	185	2.0° C.	0.800	54 ft.	0.980	108 ft.	0.920
Buffalo	181	2.2	.815	70	.965	127	.883
Boise	172	2.3	.804	70	.965	115	.907
Edmonton	181	4.1	.898	80	.958	104	.928
McGrath	156	2.5	.796	87	.980	132	.954
Frobisher	121	3.0	.867	93	.988	156	.965
Coppermine	135	2.8	.762	90	.947	159	.835

To check the results obtained from grid data, similar information from 11 radiosonde stations in North America was also processed. These stations are listed in table 5 with their standard errors of estimate, ϵ_1 , for extrapolation using station regression coefficients, and ϵ_2 , for extrap-

olation using the latitude relationship of equation (4). R^2 is also entered in this table for comparison with figures 6 and 7.

The errors associated with the station data are generally smaller than those related to the grid data, most notably in low latitudes. Outside the Caribbean region, the low-latitude zone is data-sparse, so it is evident that the process of analysis and smoothing (which filters out small-scale variations, especially where data are few) reduces the correlation. Nevertheless, the coefficients based on the smoothed data are sufficiently good that the increase in error over those using station regression coefficients is not excessive, and is indeed small compared to the difference in regression errors between station data and smoothed data. In other words, at low latitudes in particular, the values of R^2 shown in figures 6 and 7 understate the value of regression for providing point data. This is analogous to an operational situation in which a new type of observation is taken at a known latitude and extrapolated downward.

3. ESTIMATION OF THE 500-MB. TEMPERATURE

A second structure parameter at 500 mb. to be estimated from higher-level data is the temperature, T_{500} . This quantity is not as sensitive to changes in h_{300} and T_{300} as is h_{500} . In fact, results for January over an entire quadrant indicate that if h_{500} is obtained by regression and the hypsometric formula is then used in conjunction with an assumption of a constant lapse rate in the layer, the rms error in T_{500} is within 1°C. of that for the direct regression of T_{500} from h_{300} and T_{300} .

Because of this lack of sensitivity of T_{500} , T_{200} was introduced as an additional predictor. Table 6 gives the values of ϵ and R^2 for the station data, the ratios being of about the same magnitude as the estimates of h_{500} from 200-mb. parameters (table 4). The significant improvement in accuracy brought about by the inclusion of T_{200} in this regression is attributed to compensation in structural layers, T_{200} being out of phase with T_{500} .

4. SURFACE PRESSURE AS A PREDICTOR

The development of oceanic buoys with remote-sensing instrumentation poses the question, how much of the residual variance in the above regressions can be explained by ground observations? A number of 3-predictor regressions were tested, using surface pressure, p_0 , together with the predictors at 200 mb. and 300 mb. to get estimates of h_{500} and T_{500} (table 7). Since the diurnal variation of surface pressure was not removed, the low-latitude stations were excluded.

The conclusions drawn from tables 5-7 are that the utilization of p_0 will (1) generally improve the estimate of h_{500} from 300-mb. and 200-mb. predictors by a few feet at most, and (2) give almost identical results in the

regression h_{200} , T_{200} , p_0 to T_{500} as does the regression h_{300} , T_{300} , T_{200} to T_{500} . No latitudinal variation was found in these results for p_0 .

5. SUMMARY

The downward extrapolation of geopotential height and temperature data by regression from 300 mb. to 500 mb. has been shown to be feasible by use of grid data. Moreover, the regression coefficients fall into latitudinal patterns which are adequately represented by combinations of linear and parabolic curves meeting at 28° latitude. The standard error of estimate for h_{500} is typically less than 150 ft. Estimated values of h_{500} are more accurate than 24-hr. persistence estimates at all latitudes in winter. They also exceed the accuracy of 12-hr. persistence in this season, excepting at low latitudes. There is some decrease in accuracy in the other seasons.

Computed ratios of explained variance to total variance are rather close to unity in January at middle and high latitudes. The processing of radiosonde station data gives better results for h_{500} in low latitudes, suggesting that analysis noise in the 500-mb. grid data is partly responsible for the lower accuracy below 25°N.

When extrapolating from 200 mb. to 500 mb., the standard error of estimate of h_{500} is greater, the error distributions have more skewness, and extreme errors in the 400-500-ft. range occur at times. T_{500} cannot be estimated very successfully from 300-mb. information, but there is a notable increase in accuracy when T_{200} is added as a predictor. Availability of a surface pressure reading, as from a buoy platform, aids in estimating T_{500} . However, testing of January data did not reveal a combination of predictors which would permit the degree of accuracy obtainable in estimating h_{500} .

ACKNOWLEDGMENT

The financial support of Goddard Space Flight Center, NASA, under Contract Number NASr-54(08) is gratefully acknowledged.

REFERENCES

1. P. Bergthorsson and B. R. Döös, "Numerical Weather Map Analysis," *Tellus*, vol. 7, No. 3, Aug. 1955, pp. 329-340.
2. G. P. Cressman, "An Operational Objective Analysis System," *Monthly Weather Review*, vol. 87, No. 10, Oct. 1959, pp. 367-374.
3. F. G. Finger, H. M. Woolf, and C. E. Anderson, "A Method for Objective Analysis of Stratospheric Constant-Pressure Charts," *Monthly Weather Review*, vol. 93, No. 10, Oct. 1965, pp. 619-637.
4. F. F. Fischbach, "A Satellite Method for Pressure and Temperature below 24 km," *Bulletin of the American Meteorological Society*, vol. 46, No. 9, Sept. 1965, pp. 528-532.
5. L. S. Gandin, "Ob'ektivnyi Analiz Meteorologicheskikh Polei" [Objective Analysis of Meteorological Fields,] *Gidrometeorologicheskoe Izdatel'stvo*, Leningrad, 1963, 242 pp.
6. B. Gilchrist and G. P. Cressman, "An Experiment in Objective Analysis," *Tellus*, vol. 6, No. 4, Nov. 1954, pp. 309-318.

7. D. H. Johnson, "Preliminary Research in Objective Analysis," *Tellus* vol. 9, No. 3, Aug. 1957, pp. 316-322.
8. W. J. Koss, "Objective Analysis of Pressure Height Data for the Tropics," *Monthly Weather Review*, vol. 94, No. 4, Apr. 1966, pp. 237-257.
9. National Academy of Sciences, National Research Council, "The Feasibility of a Global Observation and Analysis Experiment," Pub. 1920, Washington, D.C., 1966, pp. 52-94.
10. H. A. Panofsky, "Objective Weather-Map Analysis," *Journal of Meteorology*, vol. 6, No. 6, Dec. 1949, pp. 386-392.
11. D. B. Spiegler, K. W. Veigas, and J. J. Rahn, "Objective Analysis of the Stratosphere, Based on Mid- and Upper-tropospheric Data," The Travelers Research Center Inc., Hartford, Conn., Nov. 1962.
12. S. Teweles and M. Snidero, "Some Problems of Numerical Objective Analysis of Stratospheric Constant Pressure Charts," *Monthly Weather Review*, vol. 90, No. 4, Apr. 1962, pp. 147-155.

[Received February 17, 1967; revised April 14, 1967]